JOC*Article*

# 7-Pyridylindoles: Synthesis, Structure, and Properties

Maria Salvatora Mudadu, Ajay Singh, and Randolph P. Thummel*

*Department of Chemistry, University of Houston, Houston, Texas 77204-5003*

*thummel@uh.edu*

*Received May 16, 2006*

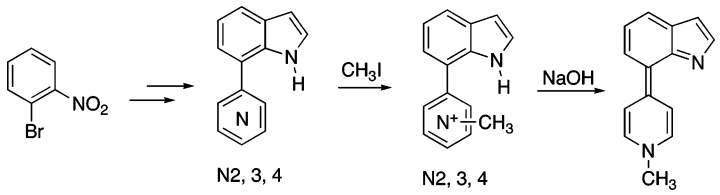


A series of three isomeric 7-pyridylindoles (7-PIs) are prepared where the pyridine attachment is through C2, C3, or C4. These systems are prepared by a combination of the Bartoli reaction and the Stille coupling with an appropriate pyridyl stannane. By treatment with $CH_3I$, the 7-PIs can be converted to their pyridinium salts. Deprotonation at the NH of these salts leads to a zwitterion which, in the 4-pyridyl system, also exists as a neutral isomer. The photophysical and NMR properties of these systems are discussed. All three pyridylindoles are analyzed by X-ray crystallography and shown to exist in different states of aggregation dictated by the formation of intra- and intermolecular H-bonds.

## Introduction

In earlier work, we have reported the preparation, properties, and tautomeric behavior of compounds related to 2-(pyrid-2′-yl)indole (**1**).[1,2] This molecule is unique for a variety of reasons, perhaps the most of important of which is that it juxtaposes a pyridine and a pyrrole. The former heterocycle is $\pi$-deficient but a good Lewis base. It also is a good H-bond acceptor. Pyrrole, on the other hand, is $\pi$-excessive, a moderate Bronsted acid, and a good H-bond donor.

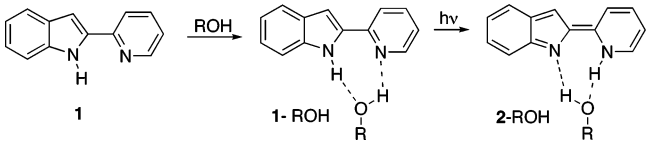


In a series of papers with Waluk and co-workers, we have examined the excited state properties of this system,[3] finding that in the excited state the basicity of the pyridine and the acidity of the pyrrole both are increased substantially. Direct photoexcited proton transfer from pyrrole to pyridine apparently does not occur largely due to the unfavorable orientation of these two moieties. Rather this process is mediated by added alcohol so that, in nonprotic solvents, **1** shows intense fluorescence which is quenched by the addition of alcohol, providing the tautomer **2**−ROH which exhibits a much weaker, lower energy emission. The direct involvement of the alcohol complex **1**−ROH in this process has been well established.[3a]

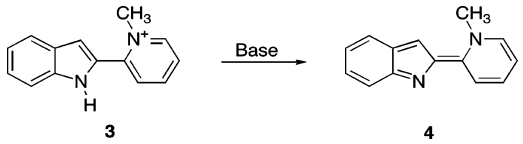


Tautomerization can be inhibited by the methylation of **1** to provide the salt **3**. With the basic pyridine site blocked, this system no longer undergoes phototautomerization. Rather treatment with base deprotonates the indole to provide **4** as a stable, well characterized species. Substituted and bridged derivatives of **3** behave in a similar fashion.[2]

The molecule 7-(pyrid-2′-yl)indole (**5**) is an isomer of **1** that is also capable of forming a proton-shifted tautomer; however, in this system, the two nitrogens have a 1,5-relationship, and the orientation of the pyridine lone pair and the pyrrole N−H is much more favorable for intramolecular H-bonding. In this study,

(1) Thummel, R. P.; Hedge, V. *J. Org. Chem.* **1989**, *54*, 1720−1725.
(2) (a) Wu, F.; Hardesty, J.; Thummel, R. P. *J. Org. Chem.* **1998**, *63*, 4055−4061. (b) Wu, F.; Chamchoumis, C. M.; Thummel, R. P. *Inorg. Chem.* **2000**, *39*, 584−590.

(3) (a) Kyrychenko, A.; Herbich, J.; Wu, F.; Thummel, R. P.; Waluk, J. *J. Am. Chem. Soc.* **2000**, *122*, 2818−2827. (b) Herbich, J.; Hung, C.; Thummel, R. P.; Waluk, J. *J. Am. Chem. Soc.* **1996**, *118*, 3508−3518. (c) Herbich, J.; Hung, C.; Thummel, R. P.; Waluk, J. *J. Photochem. Photobiol. A: Chem.* **1994**, *80*, 157−160. (d) Kyrychenko, A.; Herbich, J.; Izydorzak, M.; Gil, M.; Dobkowski, J.; Wu, F. Y.; Thummel, R. P.; Waluk, J. *Isr. J. Chem.* **1999**, *39*, 309−318. (e) Nosenko, Y.; Thummel, R. P.; Mordzinski, A. *Phys. Chem. Chem. Phys.* **2004**, *6*, 363−367.

10.1021/jo061011z CCC: $33.50 
Published on Web 09/07/2006

we have prepared and examined the series of isomeric compounds where the point of attachment of the 7-pyridyl substituent varies from 2′-pyridyl (**5**) to 3′-pyridyl (**6**) to 4′-pyridyl (**7**).

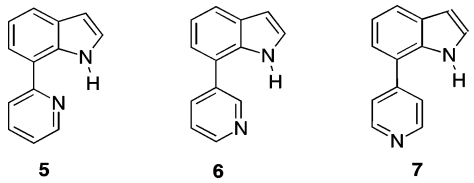


## Results and Discussion

**Synthesis and Characterization.** The 2-(pyrid-2′-yl)indole (**1**) could be readily prepared by the Fisher cyclization of the phenylhydrazone of 2-acetylpyridine.[4] This route could not be applied to the isomeric 7-pyridyl indoles, and thus we resorted to coupling methodologies. Both the 2′-pyridyl[5] and 4′-pyridyl systems could be prepared in good yield by the Stille coupling[6] between the corresponding tri-*n*-butylstannane and 7-bromoindole[7] (**8**), which was prepared by the Bartoli reaction on 2-bromonitrobenzene.[8] This coupling, however, was unsuccessful for 3-pyridyl tri-*n*-butylstannane. Alternatively, a Suzuki coupling was attempted.[9] This reaction was also unsuccessful using either 7-indolylboronic acid and 3-bromopyridine or 3-pyridylboronic acid[10] and 7-bromoindole as the coupling partners.

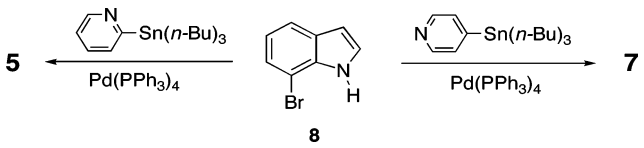


The synthesis of **6** was finally accomplished by carrying out the Stille coupling before the Bartoli reaction. Thus 3-pyridyl tri-*n*-butylstannane was coupled with 2-bromonitrobenzene to afford **10**, which was then cyclized with vinylmagnesium bromide to provide **6**.

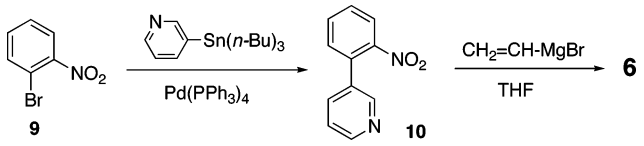


The pyridylindoles **5**−**7** were readily characterized by careful examination of their $^1$H NMR spectra, which evidenced three separate and easily identifiable spin systems for each of the three aromatic rings (Table 1). The H3 proton on the indole ring was always the highest field signal, appearing at 6.52−6.55 ppm as a doublet with a very small coupling ($J$ = 2.4−2.7 Hz) to H2. The proton adjacent to nitrogen on the pyridine ring, H6′, shows a characteristically small ($J$ = 4.2−4.5 Hz) coupling constant and thus is also readily identified, allowing one to make the remaining assignments in this ring through 2D connectivities. H4 and H6 in the benzo-ring are somewhat ambiguous and are only tentatively assigned.

**TABLE 1. $^1$H NMR Data for 7-Pyridylindoles and Their *N*-Methyl Salts[a]**

| | H2 | H3 | H4 | H5 | H6 | H2′ | H3′ | H4′ | H5′ | H6′ | $CH_3$ |
|---|---|---|---|---|---|---|---|---|---|---|---|
| **5** | 7.42 | 6.52 | 7.66 | 7.13 | 7.79 | | 8.13 | 7.91 | 7.35 | 8.76 | |
| **11** | 7.52 | 6.64 | ∼7.24 | ∼7.24 | 7.86 | | 8.15 | 8.66 | 8.22 | 9.22 | 4.00 |
| **6** | 7.34 | 6.54 | 7.60 | ∼7.14 | ∼7.14 | 8.84 | | 8.03 | 7.54 | 8.62 | |
| **12** | 7.51 | 6.62 | 7.74 | 7.20 | 7.31 | 9.35 | | 8.78 | 8.24 | 8.99 | 4.42 |
| **7** | 7.36 | 6.55 | 7.65 | 7.13 | 7.23 | 8.67 | 7.66 | | 7.66 | 8.67 | |
| **13** | 7.50 | 6.65 | 7.83 | 7.24 | 7.48 | 9.01 | 8.41 | | 8.41 | 9.01 | 4.37 |
| **14** | 7.46 | 6.33 | 7.63 | 6.78 | 7.58 | 8.65 | 9.43 | | 9.43 | 8.65 | 4.19 |

[a] Recorded in DMSO-$d_6$ at room temperature.

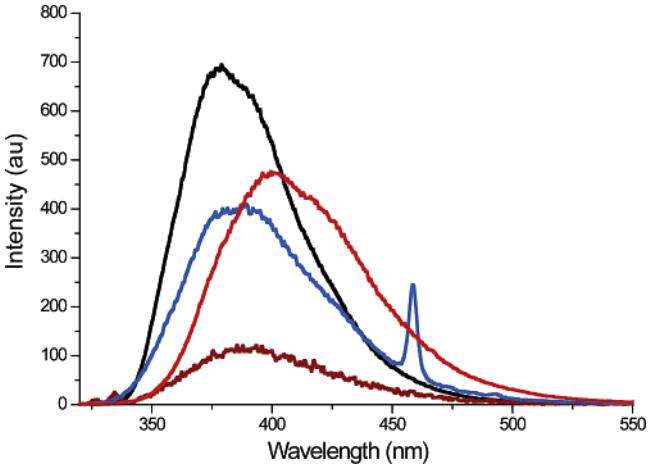


**FIGURE 1.** Emission spectra of **1** and **5**−**7** in $CH_3CN$ ($10^{-5}$ M) at room temperature with excitation at absorbance 0.12: **1** (black), **5** × 20 (brown), **6** (blue), **7** (red). Blue peak at 450 is an excitation overtone.

**Properties and Chemistry.** The most noteworthy property of the 2-(pyrid-2′-yl)indoles is their strong fluorescence in aprotic solvents.[3] This fluorescence is quenched by the addition of alcohols which form a cyclic H-bonded complex and thus assist the proton transfer step required for phototautomerization. The isomeric 7-pyridylindoles show different emissive properties. The 3′-pyridyl and 4′-pyridyl isomers **6** and **7** emit strongly at 386 and 401 nm with quantum yields of 0.25 and 0.55, respectively. The 2′-pyridyl system **5**, on the other hand, emits very weakly at 390 nm with a quantum yield of only 0.006. For this system, the fluorescence is quenched by formation of the phototautomer which is facilitated by strong intramolecular H-bonding that is impossible for the other two isomers (Figure 1). In a separate study, the detailed photophysical behavior of the three isomeric 7-pyridylindoles was examined, and the involvement of alcohol solvents in promoting fluorescence quenching of **6** and **7** has been pointed out.[11]

(4) (a) Robinson, B. *The Fischer Indole Synthesis*; Wiley: Chichester and New York, 1982. (b) Sundberg, R. J. *The Chemistry of Indole*; Academic Press: New York, 1970. (c) Thummel, R. P. *Synlett* **1992**, 1−12.

(5) Seki, K.-I.; Ohkura, K.; Terashima, M.; Kanaoka, Y. *Chem Pharm. Bull.* **1988**, *36*, 940−944.

(6) (a) Schubert, U. S.; Eschbaumer, C.; Heller, M. *Org. Lett.* **2000**, *2*, 3373−3376. (b) Littke, A. F.; Schwarz, L.; Fu, G. C. *J. Am. Chem. Soc.* **2002**, *124*, 6343−6348. (c) Fujita, M.; Oka, H. Ogura, K. *Tetrahedron Lett.* **1995**, *36*, 5247−5250.

(7) (a) Moyer, M. P.; Shiurba, J. F.; Rapoport, H. *J. Org. Chem.* **1986**, *51*, 5106−5110. (b) Leggetter, B. E.; Brown, R. K. *Can. J. Chem.* **1960**, *38*, 1467−1471. (c) Pappalardo, G.; Vitali, T. *Gazz. Chim. Ital.* **1958**, *88*, 1147.

(8) (a) Bartoli, G.; Palmieri, G.; Bosco, M.; Dalpozzo, R. *Tetrahedron Lett.* **1989**, *30*, 2129−2132. (b) Bosco, M.; Dalpozzo, R.; Bartoli, G.; Palmieri, G.; Petrini, M. *J. Chem. Soc., Perkin Trans. 2* **1991**, 657−663. (c) Dobbs, A. *J. Org. Chem.* **2001**, *66*, 638−641.

(9) (a) Carbonnelle, A.-C.; Zamora, E. G.; Beugelmans, R.; Roussi, G. *Tetrahedron Lett.* **1998**, *39*, 4467−4470. (b) Miyaura, N.; Suzuki, A. *Chem. Rev.* **1995**, *95*, 2457−2483.

(10) Cai, D.; Larsen, R. D.; Reider, P. J. *Tetrahedron Lett.* **2002**, *43*, 4285−4287.

(11) Wiosna, G.; Petkova, I.; Mudadu, M. S.; Thummel, R. P.; Waluk, J. *Chem. Phys. Lett.* **2004**, *400*, 379−383.

To more carefully examine the possible tautomeric behavior of these three species, we prepared their *N*-methyl salts in the same manner as for the conversion of **1** to **3**.[2] Treatment with a large excess of iodomethane in acetonitrile at reflux afforded the salts **11**−**13** in yields of 99, 72, and 91%, respectively. While the reaction to form **12** and **13** proceeded smoothly in 3 h, 48 h reflux was required for the formation of **11**, due to the disruption of the strong intramolecular H-bond.

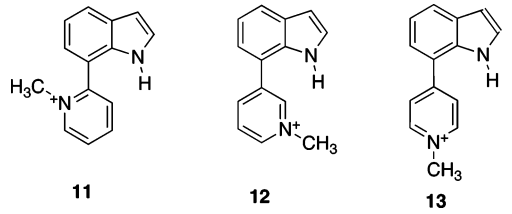


**11** **12** **13**

When a dichloromethane solution of **13** is treated with 25% NaOH for 20 min at room temperature, a deep red solid identified as the tautomer **14** is obtained in 99% yield. This observation is consistent with what was observed for the analogous 2-(pyrid-4′-yl)indole system.[2a] Treatment of **11** or **12** under similar or more severe basic conditions leads to the formation of a red solution, but a stable neutral species cannot be isolated. In all three cases, it seems likely that deprotonation occurs to initially form a zwitterion, but only in the case of **13** can the zwitterion **14a** readily undergo the electronic reorganization required to afford the isomer **14b**. For the 3′-pyridyl isomer **12**, a reasonable valence bond structure for this analogous isomer is not available. For **11**, steric interference between the *N*-methyl group and H6 or H1 causes twisting about the C7−C2′ bond that disfavors the planarity required to produce the neutral isomer.

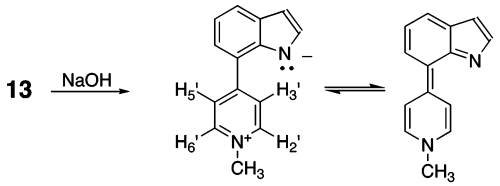


**14a** **14b**

At first glance it appears that **14a** and **14b** are resonance forms; however, due to the very different geometries of these two species, they are instead a rapidly interconverting mixture of two isomeric species. For the zwitterion **14a**, a coplanar arrangement of the indole and *N*-methylpyridinium ring would cause unfavorable steric interaction between H6 and H3′. Twisting around the 7,4′-bond relieves this interaction but also decreases conjugative interaction between the two aromatic rings.

For the 2′-pyridyl isomer **11**, this effect is magnified by the *N*-methyl group which amplifies the steric interference between the rings. The changes in the emission spectra of the 2′-pyridyl isomer **11** upon methylation and subsequent deprotonation are illustrated in Figure 2. As mentioned earlier, the normally strong indole emission is quenched in compound **5** due to the intramolecular H-bond. When this H-bond is interrupted by N-methylation, the emission increases. Deprotonation results in the appearance of a second lower energy emission band which may be attributed to the zwitterion.

These changes are even more clearly illustrated for the 4′-pyridyl isomer **13**. Figure 3 (black line) shows the absorption spectrum of an acetonitrile solution of **13**. Base is added to this

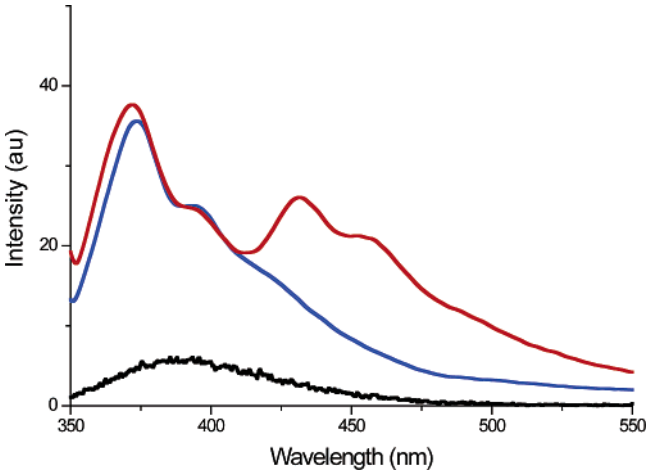


**FIGURE 2.** Emission spectra of **5** (black), **11** (red), and **11** + base (blue) $10^{-5}$ M in $CH_3CN$ at 25 °C.

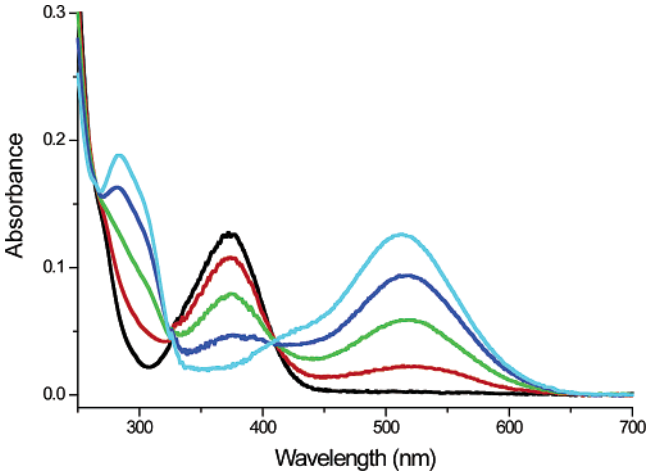


**FIGURE 3.** Electronic absorption spectra of **11** in $CH_3CN$, $10^{-5}$ M (black line); after the addition of excess KOH, 10 min (red); 20 min (blue); 30 min (dark blue); 40 min (turquoise).

solution, and the spectrum is re-measured at 10 min intervals. The absorbance of the salt at 380 nm disappears, and two new bands at 290 and 510 nm appear with clear isosbestic points, indicating a concerted conversion to the neutral species.

The same interconversion can also be monitored by $^1$H NMR. By observing the time-dependent changes in the NMR spectrum of a DMSO-$d_6$ solution of the salt **13** treated with KOH, one can follow the conversion of **13**, first to the zwitterion **14a**, and then to the neutral species **14b**. At room temperature, the two pairs of pyridinium ring protons, H3′/H5′ and H2′/H6′, appear equivalent since the isomers **14a** and **14b** are rapidly interconverting. Immediately after addition of the base, the solution becomes deep red, and the NH signal at 11.54 ppm disappears. The spectrum changes gradually with time, the most notable change being the downfield shift of H3′/H5′ and the upfield shift of H2′/H6′ (Figure 4). For the salt **13**, the pyridinium ring is twisted so that H3′ and H5′ are held over the shielding region of the adjacent indole ring and appear at higher field (8.4 ppm). Conversely, H2′ and H6′ are adjacent to the pyridinium nitrogen and are deshielded, appearing at lower field (9.0 ppm). As the salt is converted to the zwitterion **14a** and ultimately the neutral species **14b**, H3′ and H5′ move more into the deshielding region of the indole ring and downfield,

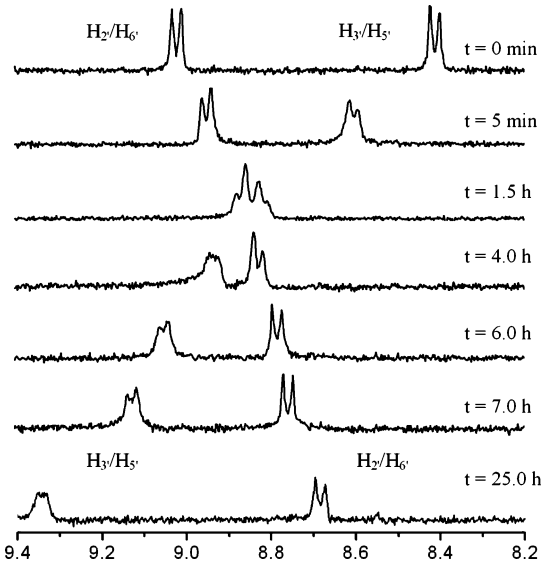


**FIGURE 4.** [1]H NMR spectra of the downfield region of **13** in DMSO-$d_6$ at room temperature, $t = 0$ min (top trace) and at time intervals after the addition of KOH.

while H2′ and H6′ experience less deshielding from the diminishing positive charge on pyridine and move upfield.

**X-ray Structures.** The structures of **5**−**7** were examined by single-crystal X-ray diffraction. Figure 5 shows the ORTEP diagrams for all three molecules, and some pertinent geometric features are summarized in Table 2. The most obvious difference between these three molecules is the dihedral angle about the C8−C10 bond which connects the two aromatic rings. For **5**, this angle is only about 3° and is explained by the strong intramolecular H-bond between N11 and N1−H, which tends to hold the two rings coplanar. Such an intramolecular H-bond is not possible for **6** and **7**, and the two aromatic rings twist out of coplanarity (ca. 54 and 65°, respectively) to relieve interactions of C7−H and N1−H with C11−H and C15−H.

The length of the C8−C10 bond also shows some significant variation for the three structures. Two opposing effects are at work. Coplanarity of the two rings would tend to increase the steric interactions mentioned earlier and thus lengthen the C8−C10 bond. At the same time, coplanarity would favor conjugative interaction between the rings which would tend to shorten the bond. It appears that the steric interactions are more influential, and thus the shortest connecting bond is found for the least planar system **7** (1.465 Å) and the longest connecting bond is for the most planar molecule **5** (1.493 Å).

The most interesting structural feature for this family of compounds is their degree of aggregation in the crystal state. This aggregation is controlled by interaction between the indole H-bond donor site and the pyridine H-bond acceptor site. For **5**, these sites are well disposed for the formation of an intramolecular H-bond, and the system is monomeric in the solid state. For **7**, the two sites are arranged in an approximate parallel fashion, and thus the molecule forms an H-bonded dimer (Figure 6, top). This dimerization leads to a large dihedral angle about the C8−C10 bond which in turn allows the two pyridine rings to lie in a stacked parallel arrangement with an interplanar distance between the two pyridines of 3.25 Å. For molecule **6**, the H-bond donor and acceptor sites are less well organized for mutual interaction, and thus the molecule forms a zigzag, polymeric H-bonded network (Figure 6, bottom).

The melting points of **5**−**7** reflect these differences in aggregation. The monomeric **5** has a relatively low mp = 65−66 °C; dimeric **7** has the highest mp = 207−208 °C, while polymeric **6** is almost exactly intermediate with mp = 130−132 °C. The shortest (1.97 Å) and most linear (174.4°) H-bond is for the polymeric system which is best able to arrange itself for favorable H-bonding, while the longest H-bond (2.08 Å) with the most acute angle (127°) is for **5** whose geometry is much more restricted.

It is well documented that H-bonding, either inter- or intramolecular, will quench the excited state emission of pyridylindoles.[12] Therefore, if the H-bonded aggregation which

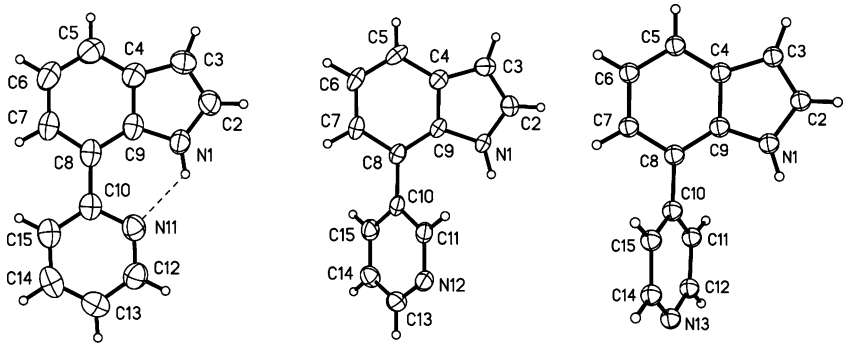


**FIGURE 5.** ORTEP plots of **5**−**7** with atom numbering scheme for X-ray discussion.

**TABLE 2. Selected Geometric Data for 7-PIs**

| bond[a] | 7-(pyrid-2′-yl)indole | 7-(pyrid-3′-yl)indole | 7-(pyrid-4′-yl)indole |
|---|---|---|---|
| C8−C10 | 1.493(4) | 1.484(4) | 1.465(6) |
| D−H | 0.90(3) | 0.94(3) | 0.87 |
| A···H | 2.08(3) | 1.97(3) | 2.06 |
| D−A | 2.719(4) | 2.882(3) | 2.925(5) |
| ∠DHA | 127°(2) | 162°(2) | 174.4° |
| C9−C8−C10−X11 | −3.0°(4) | 55.0°(4) | −65.4°(7) |
| C7−C8−C10−X15 | −3.1°(4) | 52.8°(4) | −65.3°(6) |

[a] D refers to H-bond donor (indole N), and A refers to H-bond acceptor (pyridine N).

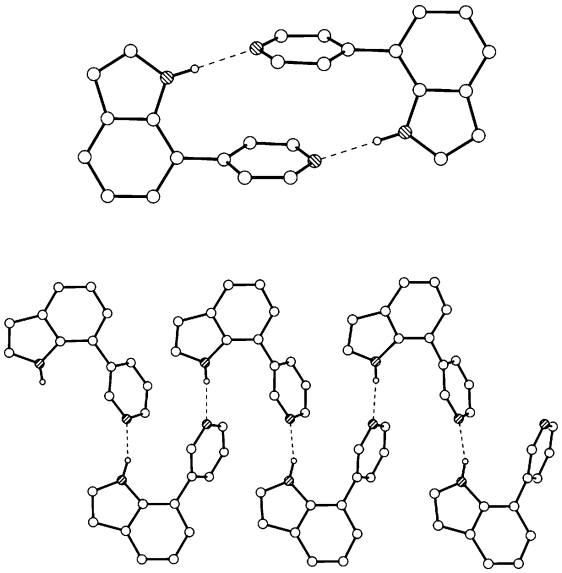

**FIGURE 6.** Organization of **6** (bottom) and **7** (top) in the crystal state.

we observe for **6** and **7** in the solid state (Figure 6) was maintained in solution, one would expect to see a similar quenching effect which might vary as a function of concentration. For **6** and **7** in acetonitrile, we observe that the emission intensity increases linearly as the concentration of the solution is increased. If H-bonded aggregation was important in solution, then we would expect to see more quenching as the concentration was increased. Apparently **6** and **7** do not aggregate significantly in relatively dilute solution.

## Experimental Section

**7-(Pyrid-2′-yl)indole (5).** A mixture of 2-tri(*n*-butylstannyl)-pyridine (80%, 5.52 g, 12.0 mmol), 7-bromoindole (**8**, 1.96 g, 10.0 mmol), and tetrakis(triphenylphosphine)palladium(0) (5 mol %, 0.58 mg, 0.50 mmol) in dry toluene (30 mL) was refluxed under Ar for 4 h. After cooling to room temperature, water (1 mL) was added and the mixture was concentrated under reduced pressure. Chromatography on silica gel, eluting with hexane, followed by $CH_2Cl_2$/hexane (1:1) provided a mixture of **5** and tri(*n*-butylstannyl)-chloride. This mixture was stored overnight in the freezer. The solid obtained was washed with hexane to provide **5** (1.62 g, 83%): mp 65−66 °C (lit.[5] mp 65−66 °C); $^1$H NMR ($CDCl_3$) $\delta$ 11.37 (br s, 1H), 8.71 (ddd, 1H, $J$ = 4.8, 2.4, 0.9 Hz), 7.03 (d, 1H, $J$ = 8.4 Hz), 7.73−7.81 (overlapping m, 3H), 7.37 (t, 1H, $J$ = 2.7 Hz), 7.19−7.25 (overlapping m, 2H), 6.61 (t, 1H, $J$ = 2.7 Hz); $^1$H NMR (DMSO-$d_6$) $\delta$ 11.62 (br s, 1H), 8.76 (d, 1H, $J$ = 4.2 Hz), 8.14 (d, 1H, $J$ = 8.4 Hz), 7.91 (td, 1H, $J$ = 8.1, 1.5 Hz), 7.80 (d, 1H, $J$ = 6.9 Hz), 7.66 (d, 1H, $J$ = 7.8 Hz), 7.42 (t, 1H, $J$ = 3.0 Hz), 7.35 (ddd, 1H, $J$ = 7.5, 4.8, 1.2 Hz), 7.13 (t, 1H, $J$ = 7.8 Hz), 6.25 (t, 1H, $J$ = 2.4 Hz); $^{13}$C NMR ($CDCl_3$) $\delta$ 158.0, 148.6, 136.8, 134.6, 129.6, 125.0, 122.6, 121.4, 120.9, 120.1, 119.5, 102.1 (one carbon hidden). Anal. Calcd for $C_{13}H_{10}N_2$: C, 80.41; H, 5.15; N, 14.43. Found: C, 80.28; H, 5.13; N, 14.36.

**7-(Pyrid-3′-yl)indole (6).** In the same manner as described for **8**, a mixture of 2-(pyrid-3′-yl)nitrobenzene (**10**, 0.32 g, 1.6 mmol), vinylmagnesium bromide (1 M, 5.3 mL, 5.3 mmol), and dry THF (17 mL) provided a crude material. Chromatography on alumina, eluting with $CH_2Cl_2$, followed by EtOAc provided **6** as a yellow solid (0.18 g, 58%), which was recrystallized from $CH_2Cl_2$/hexane: mp 130−132 °C; $^1$H NMR ($CDCl_3$) $\delta$ 10.26 (br s, 1H), 8.97 (d, 1H, $J$ = 2.1 Hz), 8.30 (dd, 1H, $J$ = 5.1, 1.8 Hz), 7.78 (dt, 1H, $J$ = 8.1, 1.8 Hz), 7.61 (d, 1H, $J$ = 7.8 Hz), 7.22 (dd, 1H, $J$ = 7.8, 5.1 Hz), 7.18 (t, 1H, $J$ = 2.7 Hz), 7.11 (d, 1H, $J$ = 7.8 Hz), 7.07 (dd, 1H, $J$ = 7.2, 1.2 Hz), 6.54 (dd, 1H, $J$ = 3.6, 2.1 Hz); $^1$H NMR (DMSO-$d_6$) $\delta$ 11.18 (br s, 1H), 8.84 (d, 1H, $J$ = 1.2 Hz), 8.62 (dd, 1H, $J$ = 4.5, 1.2 Hz), 8.03 (dt, 1H, $J$ = 8.1, 2.1 Hz), 7.60 (dd, 1H, $J$ = 7.5, 1.5 Hz), 7.54 (dd, 1H, $J$ = 7.8, 5.1 Hz), 7.34 (t, 1H, $J$ = 2.7 Hz), 7.09−7.16 (overlapping m, 2H), 7.13 (t, 1H, $J$ = 7.8 Hz), 6.254 (dd, 1H, $J$ = 2.4, 1.5 Hz); $^{13}$C NMR ($CDCl_3$) $\delta$ 149.2, 147.9, 136.4, 135.8, 134.1, 129.0, 125.5, 124.2, 122.2, 122.0, 121.1, 120.3 (one carbon hidden). Anal. Calcd for $C_{13}H_{10}N_2(1/4H_2O)$: C, 78.59; H, 5.07; N, 14.10. Found: C, 78.82; H, 5.07; N, 13.71.

**7-(Pyrid-4′-yl)indole (7).** A mixture of 4-tri(*n*-butylstannyl)-pyridine (90%, 1.27 g, 3.1 mmol), 7-bromoindole (**8**, 0.80 g, 4.1 mmol), and tetrakis(triphenylphosphine)palladium(0) (5 mol %, 18.4 mg, 0.16 mmol) in dry toluene (3 mL) was refluxed under Ar for 24 h. After cooling to room temperature, water (1 mL) was added and the mixture was concentrated under reduced pressure. Part of the product precipitated, and it was washed with $CH_2Cl_2$/hexane (1:5) and collected as a white solid (0.10 g). Chromatography of the residue on alumina, eluting with $CH_2Cl_2$ and followed by EtOAc, provided **7** as a white solid which was washed with hexane and joined to the former precipitate (0.15 g, 25%): mp 207−208 °C; $^1$H NMR (DMSO-$d_6$) $\delta$ 11.19 (br s, 1H), 8.67 (dd, 2H, $J$ = 4.2, 1.8 Hz), 7.63−7.67 (overlapping m, 3H), 7.36 (t, 1H, $J$ = 3.0 Hz), 7.22 (dd, 1H, $J$ = 7.5, 0.9 Hz), 7.13 (t, 1H, $J$ = 8.1 Hz), 6.55 (dd, 1H, $J$ = 2.7, 1.5 Hz); $^{13}$C NMR ($CDCl_3$) $\delta$ 150.1, 146.2, 132.7, 129.0, 126.4, 123.1, 122.4, 121.4, 121.1, 119.5, 101.9. Anal. Calcd for $C_{13}H_{10}N_2(1/4H_2O)$: C, 78.59; H, 5.29; N, 14.11. Found: C, 78.31; H, 5.02; N, 13.72.

**7-Bromoindole (8).** The 2-nitrobromobenzene (**9**, 1.01 g, 5.0 mmol) was placed in a two-necked round-bottom flask fitted with a gas inlet and rubber septum. The flask was purged several times with Ar before adding dry THF (50 mL) and cooling to −40 to −45 °C. Vinylmagnesium bromide (1 M, 15 mL, 15 mmol) was then added rapidly to the THF solution, and stirring continued for 1 h. Saturated $NH_4Cl$ was added to the reaction mixture at ca. −40 °C, and the mixture was allowed to warm to room temperature. The mixture was extracted with $Et_2O$ (3 × 70 mL). The combined organic phase was washed with $NH_4Cl$ (100 mL), water (100 mL), and brine (100 mL), dried ($MgSO_4$), and concentrated. Chromatography on $SiO_2$, eluting with $CH_2Cl_2$, provided **8** as a white solid (0.52 g, 53%): mp 42−44 °C (lit.[6b] mp 42−43 °C); $^1$H NMR ($CDCl_3$) $\delta$ 8.33 (s, 1H), 7.58 (d, 1H, $J$ = 7.8 Hz), 7.34 (d, 1H, $J$ = 7.8 Hz), 7.25 (m, 1H), 7.00 (t, 1H, $J$ = 7.8 Hz), 6.63 (dd, 1H, $J$ = 3.3, 2.4 Hz).

**2-(Pyrid-3′-yl)nitrobenzene (10).** A mixture of 3-tri(*n*-butylstannyl)pyridine (0.42 g, 1.1 mmol), 2-nitrobromobenzene (**9**, 0.20 g, 1.0 mmol), and tetrakis(triphenylphosphine)palladium(0) (5 mol %, 57.8 mg, 0.05 mmol) in dry toluene (3 mL) was refluxed under Ar for 21 h. After cooling to room temperature, water (1 mL) was added. The solvent was removed under reduced pressure. Chromatography on alumina, eluting with hexane, then with $CH_2Cl_2$ furnished **10** as a yellow oil (0.17 g, 83%): $^1$H NMR ($CDCl_3$) $\delta$ 8.68 (dd, 1H, $J$ = 5.1, 1.5 Hz), 8.62 (d, 1H, $J$ = 1.8 Hz), 8.03 (dd, 1H, $J$ = 8.1, 0.9 Hz), 7.69−7.74 (overlapping m, 2H), 8.68 (td, 1H, $J$ = 8.1, 1.5 Hz), 8.62 (d, 1H, $J$ = 1.8 Hz), 7.42−7.46 (overlapping m, 2H).[13]

**1-Methyl-2-(indol-7′-yl)pyridinium iodide (11).** A solution of iodomethane (1.6 mL, 25.7 mmol) in $CH_3CN$ (3 mL) was added dropwise, during a period of 6 h, to a boiling solution of 7-(pyrid-2′-yl)indole (**5**, 0.49 g, 2.5 mmol) in $CH_3CN$ (3 mL) under Ar. The yellow mixture was refluxed for 48 h. After cooling to room temperature, the solvent was evaporated and the yellowish solid dried to furnish pure **11** (0.85 g, 99%): mp 205−207 °C; $^1$H NMR (DMSO-$d_6$) $\delta$ 11.31 (br s, 1H), 9.22 (d, 1H, $J$ = 5.7 Hz), 8.66 (dd,

(12) (a) Herbich, J.; Rettig, W.; Thummel, R. P.; Waluk, J. *Chem. Phys. Lett.* **1992**, *195*, 556−562. (b) Herbich, J.; Waluk, J.; Thummel, R. P.; Hung, C.-Y. *J. Photochem. Photobiol. A: Chem.* **1994**, *80*, 157−160.

(13) Cioffi, C. L.; Spencer, W. T.; Richards, J. J.; Herr, R. J. *J. Org. Chem.* **2004**, *69*, 2210−2212 (S24).

**TABLE 3. Data Collection and Processing Parameters for 7-Pyridylindoles**

| compound | 7-(pyrid-2′-yl)indole | 7-(pyrid-3′-yl)indole | 7-(pyrid-4′-yl)indole |
|---|---|---|---|
| molecular formula | $C_{13}H_{10}N_2$ | $C_{13}H_{10}N_2$ | $C_{13}H_{10}N_2$ |
| formula weight | 194.23 | 194.23 | 194.23 |
| space group | $P2_1/c$ (orthorhombic) | $P\bar{1}$ (triclinic) | $P2_1/c$ (monoclinic) |
| cell constants | $A = 9.7196(7)$ Å | $A = 7.3185(11)$ Å | $A = 15.3107(14)$ Å |
| | $B = 17.4764(13)$ Å | $B = 10.6790(15)$ Å | $B = 7.6895(7)$ Å |
| | $C = 11.7484(9)$ Å | $C = 14.4363(21)$ Å | $C = 18.4142(18)$ Å |
| | $\alpha = 90.00°$ | $\alpha = 72.415(2)°$ | $\alpha = 90.00°$ |
| | $\beta = 90.00°$ | $\beta = 87.546(2)°$ | $\beta = 112.269(2)$ |
| | $\gamma = 90.00°$ | $\gamma = 70.876(2)°$ | $\gamma = 90.00°$ |
| formula units per cell | $Z = 8$ | $Z = 4$ | $Z = 8$ |
| volume | 1995.6(3) Å$^3$ | 1014.2(3) Å$^3$ | 2006.2(3) Å$^3$ |
| density | $\rho = 1.293$ mg/m$^3$ | $\rho = 1.272$ mg/m$^3$ | $\rho = 1.286$ mg/m$^3$ |
| absorption coefficient | $\mu = 0.078$ mm$^{-1}$ | $\mu = 0.077$ mm$^{-1}$ | $\mu = 0.078$ mm$^{-1}$ |
| temperature | 223(2) K | 223(2) K | 223(2) K |
| radiation (Mo Kα) | $\lambda = 0.71073$ Å | $\lambda = 0.71073$ Å | $\lambda = 0.71073$ Å |
| scan speed range | 1.17−22.51° min$^{-1}$ | 1.48−23.56° min$^{-1}$ | 1.44−23.49° min$^{-1}$ |
| total data collected | 8483 | 4675 | 9312 |
| independent data | 2473 | 2976 | 3229 |
| total variables | 278 | 278 | 278 |
| *R*1 | 0.0259 | 0.0494 | 0.0658 |
| *wR* or *wR*2 | 0.0660 | 0.1299 | 0.1765 |

1H, $J = 7.8$, 6.9 Hz), 8.22 (t, 1H, $J = 5.7$ Hz), 8.15 (d, 1H, $J = 7.8$ Hz), 7.22 (dd, 1H, $J = 7.8$, 5.1 Hz), 7.85 (dd, 1H, $J = 7.2$, 2.1 Hz), 7.52 (t, 1H, $J = 2.4$ Hz), 7.21−7.29 (overlapping m, 2H), 6.64 (dd, 1H, $J = 3.6$, 2.1 Hz), 4.01 (s, 3H); $^1$H NMR ($CD_3CN$) $\delta$ 9.97 (br s, 1H), 8.87 (d, 1H, $J = 6.0$ Hz), 8.54 (td, 1H, $J = 7.8$, 0.9 Hz), 8.07 (t, 1H, $J = 5.7$ Hz), 8.04 (d, 1H, $J = 7.5$ Hz), 7.90 (d, 1H, $J = 6.9$ Hz), 7.37 (t, 1H, $J = 3.0$ Hz), 7.28 (t, 1H, $J = 6.9$ Hz), 7.23 (dd, 2H, $J = 7.5$, 1.5 Hz), 6.67 (dd, 1H, $J = 3.0$, 1.5 Hz), 4.03 (s, 3H); $^{13}$C NMR ($CDCl_3$) $\delta$ 148.0, 146.8, 133.8, 132.0, 130.2, 128.1, 127.5, 125.0, 123.8, 120.5, 118.1, 115.9, 103.6, 47.5.

**1-Methyl-3-(indol-7′-yl)pyridinium iodide (12).** In the same manner described above for **11**, a solution of iodomethane (1.13 g, 8.0 mmol) in $CH_3CN$ (2 mL) and a solution of 7-(pyrid-3′-yl)-indole (**6**, 0.15 g, 0.8 mmol) in $CH_3CN$ (2 mL) provided a crude material after refluxing for 3 h. Chromatography on alumina, eluting with $CH_3CN$, provided a yellow solid, which was washed with hexane to furnish **12** (0.19 g, 72%): mp 209−211 °C; $^1$H NMR (DMSO-$d_6$) $\delta$ 11.46 (br s, 1H), 9.35 (s, 1H), 8.99 (d, 1H, $J = 6.0$ Hz), 8.79 (d, 1H, $J = 8.4$ Hz), 8.24 (t, 1H, $J = 7.2$ Hz), 7.74 (d, 1H, $J = 7.8$ Hz), 7.51 (t, 1H, $J = 3.0$ Hz), 7.31 (d, 1H, $J = 7.2$ Hz), 7.21 (t, 1H, $J = 8.1$ Hz), 7.51 (s, 1H), 4.42 (s, 3H); $^{13}$C NMR (DMSO-$d_6$) $\delta$ 145.1, 144.2, 143.4, 138.0, 132.8, 129.0, 127.7, 126.7, 122.2, 122.1, 119.6, 118.0, 102.1, 48.03.

**1-Methyl-4-(indol-7′-yl)pyridinium iodide (13).** In the same manner described above for **11**, a solution of iodomethane (0.85 g, 6.0 mmol) in $CH_3CN$ (2 mL) and a solution of 7-(pyrid-4′-yl)-indole (**7**, 0.12 g, 0.6 mmol) in $CH_3CN$ (6 mL) provided a yellow pure **13** after refluxing for 3 h (0.18 g, 91%): mp 213-215 °C; $^1$H NMR (DMSO-$d_6$) $\delta$ 11.54 (br s, 1H), 9.02 (d, 2H, $J = 6.9$ Hz), 8.41 (d, 2H, $J = 6.6$ Hz), 7.83 (t, 1H, $J = 8.1$ Hz), 7.47−7.50 (overlapping m, 2H), 7.24 (t, 1H, $J = 8.1$ Hz), 6.65 (m, 1H), 4.37 (s, 3H); $^{13}$C NMR ($CDCl_3$) $\delta$ 153.8, 145.2, 132.5, 129.6, 127.2, 126.1, 124.2, 123.1, 119.8, 119.1, 102.4, 47.1.

**1-Methyl-4-(indolen-4′-ylene)-1,2-dihydropyridine (14).** A suspension of **13** (80 mg, 2.4 mmol) in $CH_2Cl_2$ (10 mL) and 25% NaOH (10 mL) was stirred at room temperature for 20 min. The two phases were separated, and the aqueous phase was extracted with $CH_2Cl_2$ (4 × 20 mL). The combined phase was washed with 10% NaOH (5 mL), dried ($Na_2CO_3$) under vigorous stirring for 30 min, and concentrated to provide **14c** as a deep red solid (50 mg, 99%): mp 84−86 °C; $^1$H NMR (DMSO-$d_6$) $\delta$ 9.43 (d, 2H, $J = 7.5$ Hz), 8.64 (d, 2H, $J = 6.6$ Hz), 7.63 (d, 1H, $J = 7.5$ Hz), 7.58 (d, 1H, $J = 6.9$ Hz), 7.46 (d, 1H, $J = 1.8$ Hz), 6.78 (t, 1H, $J = 8.1$ Hz), 6.33 (d, 1H, $J = 2.4$ Hz), 4.19 (s, 3H).

**X-ray Structure Determinations.** All measurements were made with a Siemens SMART platform diffractometer equipped with a 1K CCD area detector. A hemisphere of data (1271 frames at 5 cm detector distance) was collected using a narrow-frame method with scan widths of 0.30° in omega and an exposure time of 30 s/frame. The first 50 frames were re-measured at the end of data collection to monitor instrument and crystal stability, and the maximum correction on $I$ was <1%. The data were integrated using the Siemens SAINT program, with the intensities corrected for Lorentz factor, polarization, air absorption, and absorption due to variation in the path length through the detector faceplate. A psi scan absorption correction was applied based on the entire data set. Redundant reflections were averaged.

**7-(Pyrid-2′-yl)indole (5).** Final cell constants were refined using 3739 reflections having $I > 10\sigma(I)$, and these, along with other information pertinent to data collection and refinement, are listed in Table 3. The Laue symmetry was determined to be *mmm*, and from the systematic absences noted the space group was shown to be either *Pca*2(1) or *Pbcm*. The asymmetric unit consists of two independent molecules. The hydrogens attached to N were allowed to refine freely.

**7-(Pyrid-3′-yl)indole (6).** Final cell constants were refined using 2195 reflections having $I > 10\sigma(I)$, and these, along with other information pertinent to data collection and refinement, are listed in Table 3. The Laue symmetry was determined to be −1, and the space group was shown to be either $P1$ or $P\bar{1}$. The asymmetric unit consists of two independent molecules having small but significant differences in geometry. Hydrogens attached to nitrogen were refined independently.

**7-(Pyrid-4′-yl)indole (7).** Final cell constants were refined using 2831 reflections having $I > 10\sigma(I)$, and these, along with other information pertinent to data collection and refinement, are listed in Table 3. The Laue symmetry was determined to be 2/*m*, and from the systematic absences noted the space group was shown unambiguously to be $P2(1)/c$. There are two independent molecules per asymmetric unit, both forming hydrogen-bonded pairs with their symmetry relative across an inversion center. One of the molecules was found to be disordered approximately 5:1 with its mirror image (ignoring the torsional twist of the pyridyl ring), and this was treated by refinement of two ideal rigid bodies for the minor component. Due to the close proximity of many of the atoms in the two orientations, all atoms were refined isotropically.

**Acknowledgment.** We thank the Robert A. Welch Foundation (E-621) and the National Science Foundation (CHE-0352617) for financial support. We would also like to thank Dr. James Korp for assistance with the X-ray determinations which made use of MRSEC/TCSUH shared facilities supported by the NSF (DMR-9632667) and the Texas Center for Superconductivity at the University of Houston.

**Supporting Information Available:** X-ray crystallographic data (CIF files) for **5**−**7**, general experimental methods, $^{1}$H and $^{13}$C NMR spectra for **11**−**13**, and $^{1}$H NMR spectrum for **14**. This material is available free of charge via the Internet at http://pubs.acs.org.

JO061011Z